Nutrition, Metabolism & Cardiovascular Diseases (2019) **29**, 639–651

Available online at www.sciencedirect.com

Nutrition, Metabolism & Cardiovascular Diseases

journal homepage: www.elsevier.com/locate/nmcd

Notch3 signaling activation in smooth muscle cells promotes extrauterine growth restriction-induced pulmonary hypertension

Y. Wang [a], S. Dai [a], X. Cheng [a], E. Prado [b], L. Yan [a], J. Hu [c], Q. He [d], Y. Lv [a], Y. Lv [a], L. Du [a,*]

[a] Department of Pediatrics, Children's Hospital of Zhejiang University School of Medicine, Hangzhou, China
[b] Loma Linda University School of Medicine, Loma Linda, CA, USA
[c] Department of Surgical Intensive Care Unit, Second Affiliated Hospital of Zhejiang University, Hangzhou, China
[d] Department of Pediatrics, West China Second University Hospital, Sichuan University, Chengdu, China

Received 22 January 2019; received in revised form 1 March 2019; accepted 4 March 2019
Handling Editor: Gian Luigi Russo
Available online 13 March 2019

KEYWORDS
Pulmonary hypertension;
Extrauterine growth restriction;
Pulmonary artery smooth muscle cells;
Notch3 signaling pathway

Abstract *Background and aims:* Early postnatal life is a critical developmental period that affects health of the whole life. Extrauterine growth restriction (EUGR) causes cardiovascular development problems and diseases, including pulmonary arterial hypertension (PAH). PAH is characterized by proliferation, migration, and anti-apoptosis of pulmonary artery smooth muscle cells (PASMCs). However, the role of PASMCs in EUGR has not been studied. Thus, we hypothesized that PASMCs dysfunction played a role in EUGR-induced pulmonary hypertension.
Methods and results: Here we identified that postnatal nutritional restriction-induced EUGR rats exhibited an elevated mean pulmonary arterial pressure and vascular remodeling at 12 weeks old. PASMCs of EUGR rats showed increased cell proliferation and migration features. In EUGR-induced PAH rats, Notch3 signaling was activated. Relative mRNA and protein expression levels of Notch3 intracellular domain (Notch3 ICD), and Notch target gene Hey1 in PASMCs were upregulated. We further demonstrated that pharmacological inhibition of Notch3 activity by using a γ-secretase inhibitor DAPT, which blocked the cleavage of Notch proteins to ICD peptides, could effectively inhibit PASMC proliferation. Specifically knocked down of Notch3 in rat PASMCs by shRNA restored the abnormal PASMC phenotype *in vitro*. We found that administration of Notch signaling inhibitor DAPT could successfully reduce mean pulmonary arterial pressure in EUGR rats.
Conclusions: The present study demonstrated that upregulation of Notch3 signaling in PASMCs was crucial for the development of EUGR-induced PAH. Blocking Notch3-Hey1 signaling pathway in PASMCs provides a potential therapeutic target for PAH.

Abbreviations: EUGR, extrauterine growth restriction; PAH, pulmonary arterial hypertension; PASMCs, pulmonary artery smooth muscle cells; Notch3 ICD, Notch3 intracellular domain; PAEC, pulmonary arterial endothelial cells; RV, right ventricular; LV, left ventricle; RVHI, right ventricular hypertrophy index; mPAP, mean pulmonary arterial pressure; shRNA, short hairpin RNA; ANOVA, one-way analysis of variance.

* Corresponding author. Department of Neonatology, Children's Hospital of Zhejiang University, Hangzhou 310052, China.
E-mail address: dulizhong@zju.edu.cn (L. Du).

https://doi.org/10.1016/j.numecd.2019.03.004
0939-4753/

Introduction

Early postnatal life is a critical developmental period for determining organ function and long-term metabolic status [1]. Extrauterine growth restriction (EUGR) remains a serious problem in very low birth weight infants and is a manifestation of severe malnutrition in the first few weeks of life [2]. EUGR is associated with a higher risk of long-term cardiovascular diseases including pulmonary hypertension [3–7]. Dysfunction of pulmonary vascular endothelial cells has been identified in EUGR-induced pulmonary hypertension in adulthood [8,9]. However, the role and mechanism of pulmonary artery smooth muscle cells (PASMCs) of EUGR and pulmonary hypertension are still unclear.

Pulmonary arterial hypertension (PAH) is a severe and progressive disease. The remodeling of pulmonary arterioles results in increased pulmonary vascular resistance, elevated mean pulmonary artery pressure, right ventricular failure or death [10]. It is pathologically characterized by proliferation, migration, anti-apoptosis, or phenotype switching of pulmonary arterial endothelial cells (PAEC), PASMCs, and fibroblasts [11–13]. Multiple etiologies account for PAH, but the mechanism of pulmonary hypertension due to developmental lung diseases remains unclear [14]. Thus, we explore the mechanism of PAH from the perspective of EUGR-induced pulmonary arterial hypertension, and this might provide a new potential solution for PAH.

Increasing evidence suggests that Notch3 is activated in pulmonary hypertension (PH) [15,16]. Notch3 is the major Notch receptor in vascular smooth muscle cells, and is critical in determining the lineage fate of the of vascular smooth muscle cells (SMC) in late embryonic development [17]. Notch receptors (Notch1–4) are single-pass transmembrane proteins that receive signals from ligands encoded by the Jag (Jag1, Jag2) and Delta-like (Dll1, Dll3, and Dll4) gene families [18]. After ligand binding, Notch receptors undergo several proteolytic events mediated by a succession of proteases (including γ-secretases), result in releasing of the intracellular domains (ICD) of these receptors [19]. The Notch ICD translocates to the nucleus to form an active transcriptional complex with transcription factor to activate the transcription of effector genes. The key downstream genes of Notch signaling are the Hes/Hey families, which have been shown to function as downstream of notch receptors in many organs [20]. Blockade of the Notch pathway using the γ-secretase inhibitor N-[N-(3,5-diflurophenacetyl)-L-alanyl]-S-phenylglycinetbutyl ester (DAPT) which blocked the cleavage of Notch proteins to ICD peptides could be a valuable approach for the therapy of PAH [6].

Since the function of PASMCs in EUGR has not been studied, we hypothesize that EUGR induced pulmonary hypertension is related to dysfunction of PASMCs, possibly through Notch pathway. Here we show that Notch3 is implicated in the development of PAH *in vitro* and *in vivo* EUGR models. Inhibition or knockdown of Notch3 leads to reversing of the hyperproliferative phenotype of PASMCs in PAH. Thus, our findings identify that Notch3 is centrally involved in EUGR-induced PAH, and provide new insights into its role in pulmonary hypertension.

Methods

Extrauterine growth restriction rat model

This study was carried out in accordance with the recommendations of the National Institutes of Health Guidelines for the Care and Use of Laboratory Animals of the National Institutes of Health. The procedures and protocols were approved by the Animal Care and Use Committee of Zhejiang University (No. ZJU20160215). All surgery was carried out under anesthesia, and all efforts were aimed at reducing pain. *Sprague–Dawley* rats obtained from Zhejiang Chinese Medical University Laboratory Animal Center and were kept in the same room with a constant temperature maintained at 22–24 °C, and allowed to drink water freely.

The EUGR rat model was set up as described in our previous study [8]. Briefly, pregnant *Sprague–Dawley* rats maintained a standard diet throughout gestation. Within 24 h after birth, pups were weighed and randomly allocated to either a control litter consisting of 10 pups, or a large litter consisting of 20 pups, both with a 1:1 male-to-female ratio. This model has been demonstrated to produce equal growth restriction in each of the pups of the large litter [21]. Pups were weaned on postnatal day 21 and male rats were housed four per cage until 12 weeks of age. Weighing less than the 10th percentile of age-matched controls were considered as EUGR [22]. Offspring were weighed once a week thereafter until 12 weeks old. To avoid the variability of the results related to the hormonal cycle in female rats, only male offspring were studied.

DAPT treatment of rats

EUGR and control rats were randomized to receive a dose of 10 mg/kg [15,16] of the γ-secretase inhibitor, DAPT (D5942, Sigma–Aldrich, St. Louis, MO, USA) or an equivalent volume of vehicle (DMSO) at 48 h before sacrificed at 12 weeks old.

Hemodynamic and right ventricular (RV) hypertrophy measurements

To measure the mean pulmonary arterial pressure (mPAP), 12 weeks old rats were anesthetized with 2% pentobarbital (50 mg/kg, i.p.) and placed on a thermo-regulated surgical table, connected to a small-animal ventilator. A PE-50 catheter was inserted from the right jugular vein through the right heart into the main pulmonary artery. Placement at each stage was confirmed by respective pressure contours. Data were measured and analyzed by physiological data acquisition system (Acknowledge MP150; Biopac System Inc., Goleta, California, USA).The rats were then sacrificed, and the hearts and lungs were collected.

To evaluate the extent of RV hypertrophy, the right ventricle was dissected from the left ventricle (LV) and interventricular septum (S) and weighed separately. The right ventricular hypertrophy index (RVHI) was calculated by the formula: RVHI (%) = [RV/(LV + S)] × 100.

Assessment of vascular remodeling in vivo

Lungs were fixed in 10% buffered formalin, embedded in paraffin, and sectioned at 4–5 μm thickness. For immunostaining, the anti-actin, α-smooth muscle (α-sma) (A2547 Sigma–Aldrich, St. Louis, MO, USA; 1:400 dilution) was used to differentiate the media of pulmonary arterioles. Images of pulmonary arterioles smaller than 100 μm in diameter and adjacent to alveolar ducts were captured with an Olympus microscope digital camera system (Olympus, Tokyo, Japan). Pulmonary vascular remodeling was evaluated by measuring the percentage of pulmonary arterial medial thickness occupied by smooth muscle. Pulmonary arterioles were measured using the Image Pro Plus 5.1 image analysis program (Media Cybernetics, Silver Spring, MD). Multiple lung sections were made for each rat and >20 vessels were analyzed in each lung section.

Real-time quantitative PCR (RT-PCR)

Total mRNA was extracted from frozen rat lung tissues and PASMCs using an AxyPrep Total RNA Miniprep Kit (Axygen, Union City, USA). Equal amounts of isolated RNA were subsequently transcribed into cDNA using the reverse transcriptase kit (Takara, Kusatsu, Japan) according to the manufacturer's instructions. Synthesized cDNA was analyzed by real-time PCR using the StepOnePlus Real Time PCR System with SYBR-Green protocol (Takara, Kusatsu, Japan). Conditions for RT-PCR was at 95 °C/30 s, 56–60 °C/60 s, 60 °C/30 s. The primers sequences used in this study were shown in Supplementary Table 1. Relative expression of each target gene was analyzed with the $2^{-(\Delta(\Delta Ct))}$ method. Target gene expression was normalized to β-actin.

Western blot and quantification

Lung tissue samples or cellular samples prewashed with cold PBS were homogenized in lysis buffer (RIPA buffer and protease inhibitors) and centrifuged for 20 min at 12,000*g*. Lysates were separated on 8% polyacrylamide gels and transferred to polyvinylidene difluoride membranes. Membranes were then blocked and probed with one of the following primary antibodies: Rabbit polyclonal anti-Notch3 (catalog number: ab23426; 1:500 dilution, Abcam, Cambridge, UK), Rabbit polyclonal anti-HEY1 (ab154077, 1:250 dilution, Abcam, Cambridge, UK), Goat polyclonal anti-Jag 1 (J4127, 1:500 dilution, Sigma–Aldrich, St. Louis, MO, USA), Mouse monoclonal anti-α-Tubulin as a loading control (T6074, 1:5000 dilution, Sigma–Aldrich, St. Louis, MO, USA). After washing, the membranes were incubated with secondary antibodies conjugated with horseradish peroxidase (HRP) for 1 h at room temperature. Bound antibodies were detected by SuperSignal West Pico Chemiluminescent Substrate (Thermo Scientific, Hanover Park, IL, USA) and the blots were visualized by using the G:BOX gel doc system (Syngene, Frederick, MD, USA). Expression was quantified by densitometry normalized to α-Tubulin using Image J software.

Notch3 immunofluorescence staining in lung tissues

Paraffin-embedded lung tissue was deparaffinized in xylene and rehydrated in a graded ethanol series to PBS, followed by antigen retrieval. Double immunofluorescence staining was performed with primary antibodies to Rabbit polyclonal anti-NOTCH3 (catalog number: ab23426; 1:250 dilution, Abcam, Cambridge, UK), mouse monoclonal anti-α-SMA antibody (1:400, A2547, Sigma, Saint Louis, MO). After 4 °C overnight incubation, slides were washed with PBS and further incubated for 1 h with respective secondary antibodies, Alexa 488 conjugated goat anti-mouse IgG (1:800 dilution, ab150117, Abcam, Cambridge, UK) and Alexa 594 conjugated goat anti-rabbit IgG (1:800 dilution, ab150080). Nuclei were counterstained with DAPI. Fluorescent signals were detected using Nikon Eclipse C1 microscope (Nikon, Tokyo, Japan) and 3D Histech software (3DHISTECH Ltd, Budapest, Hungary).

Rat primary PASMC culture

Rat primary PASMCs were isolated and cultured from peripheral small pulmonary artery of EUGR or control ($n = 8$ each). Pulmonary arterial segments were cut to expose the luminal surface. To get the media, the endothelium was removed by gentle scraping and the adventitial layer was peeled away. After washing with Hank's balanced salt solutions (HBSS), the medial explants were cut into 1–2 mm^2 sections, digested using papain and collagenase (all from Sigma–Aldrich, St. Louis, MO, USA) dissolved in HBSS at 37 °C for 20 min. The sample was centrifuged and resuspended in DMEM. PASMCs were collected through centrifugation at 2000*g* for 10 min and cultured with DMEM high glucose containing 20% fetal bovine serum (FBS) and 1% antibiotics (Gibco/Invitrogen, USA) until cells had formed confluent monolayers. PASMCs were trypsinized, and the subsequent passages were cultured in DMEM containing 15% FBS and antibiotics in 5% CO_2 in air at 37 °C. PASMCs from passages 3 or 4 were used for all experiments.

PASMCs treatment with NOTCH pathway inhibitor DAPT

Rat PASMCs were incubated in serum-free medium for 24 h and then received either the γ-secretase inhibitor, DAPT (D5942, Sigma–Aldrich, St. Louis, MO, USA) at the corresponding concentration or 0.1% DMSO for 48 h. After 48 h, cells were assessed for proliferation and harvested for RT-PCR or western blot. The concentration and incubation time of the compounds were based on previous studies [16] and preliminary experiments.

Knocking down of Notch3 by lentiviral short hairpin RNA (shRNA)

The following Notch3-targeted short hairpin RNAs were designed and synthesized by Genechem Co. Ltd (Shanghai, China). Viruses were amplified and titrated in 293T cells according to manufacturer's instructions. To knockdown Notch3, rat PASMCs were plated at 50% confluency transduced with 40 MOI Notch3 shRNA (1#: 5′-CACCTGCAACCCGGTTTATAA-3′; 2#: 5′-GACCGTGTGGCCTCTTTCTAT-3′) or scramble shRNA (5′-TTCTCCGAACGTGTCACGT-3′) packaged in lentiviral transduction particles. The viruses were used to infect cells for 16 h in the presence of viral infection enhancer HitransG P and then changed to normal serum-containing medium. Cells were grown for an additional 48 h and were used for PCR or western blotting to confirm knockdown.

Assessment of proliferation of PASMCs

PASMC proliferation was assessed with BrdU colorimetric incorporation assay (Roche Diagnostics GmbH, Mannheim, Germany). PASMCs were seeded at 5000 cells per well into 96-well microplates and treated with different drugs. Cells were incubated in serum-free medium for 24 h and then labeled with BrdU for 2 h and incubated with FixDenat solution for 30 min. Cells were immunostained with anti-BrdU-POD for 90 min, washed three times with PBS, and reacted with substrate solution for 30 min. The reaction product is quantified by measuring the absorbance at the respective wavelength using an ELISA reader (Tecan, Switzerland) with 370 nm filter and 492 nm as reference wavelength.

Apoptosis analysis

Cell apoptosis was evaluated by flow cytometry using the Annexin V/PI staining kit (BD Biosciences, 556547). Cells were trypsinized and collected, and resuspended in 100 μL 1× binding buffer. After incubation with 5 μL Annexin V-FITC and 5 μL propidium iodide (PI) for 15 min at 25 °C in the dark, added 200 μL 1× binding buffer to each tube and analyzed by flow cytometry (FACScan, Becton Dickinson, CA, USA).

PASMC apoptosis was also assessed with One Step TUNEL Apoptosis Assay Kit (Beyotime, China) according to the manufacturer's instructions. Cells were fixed with 4% paraformaldehyde for 30 min, followed by rinsing with PBS. Then the cells were permeabilized with 0.3% Triton X-100 in PBS at room temperature for 5 min, and rinsed with PBS. Cells were then incubated with Terminal Deoxynucleotidyl Transferase and fluorescein-dUTP for 1 h at 37 °C. The FITC-labeled TUNEL-positive cells were then imaged using Zeiss VivaTome microscope (Axioscan Z1-Zeiss, Jena, Germany) and cells labeled with FITC were counted.

Migration assay

Wound injury was made with a p200 pipette tip to create a 'scratch' and detached cells were washed with PBS. Cells were then incubated and migrated for 24 h. Wound closure was quantified by the percent change of wound area. Migration index = [(initial wound width − width of wound at time point tested)/initial wound width]*100%.

The influence on PASMC migration and invasion was also assessed with Transwell chamber migration assay. A Transwell chamber assay was performed using a 24-well transwell insert (8 mm pore size) (Coster) pre-coated with BD Matrigel matrix (BD Biosciences). The lower chamber was filled with 10% FBS as a chemoattractant. Cells were incubated in serum-free medium, and 1×10^5 cells were added into the upper chamber. After 24 h incubation, non-invaded cells were rubbed off from the upper chamber. The invaded cells remaining on the lower surface of the insert were fixed and stained with crystal violet. Cells were quantified as the average number found in five random microscopic fields in three independent experiments.

Statistical analysis

Data were presented as mean ± S.E.M. All experiments were performed at least three times. Statistical differences were assessed using Student's *t* test for comparisons between two groups, and one-way analysis of variance (ANOVA) and Newman−Keuls post-hoc test for multiple group analysis. The number of animals/samples in each group was shown in the figure legends. $^*P$ values <0.05 was considered significant. All statistical analyses were performed using Prism 5.0 (GraphPad Software, La Jolla, CA).

Results

Extrauterine growth restriction male rats developed increased pulmonary artery pressure and pulmonary arteriolar remodeling

EUGR rat model was set up as Fig. 1a. On the first day, there was no significant difference of body weight between EUGR and control group. Then after the group was assigned, the weight of EUGR group was much lower than that of control group (Fig. 1b), which showed that the model of EUGR had been successfully constructed. To explore whether EUGR induces pulmonary vascular dysfunction, we assessed hemodynamics and pulmonary vascular remodeling of EUGR rats. Compared with control, EUGR rats exhibited an elevated mean Pulmonary Arterial Pressure (mPAP) (Fig. 1c). Weight of right ventricular to that of the left ventricle and septum, as an index of right ventricular hypertrophy, was significantly increased in EUGR rats (Fig. 1d). For immunostaining, α-smooth muscle (α-sma) was used to differentiate the media of pulmonary arterioles. Similarly to the observed hemodynamic changes, EUGR rats exhibited increased pulmonary arterial medial thickness (Fig. 1e and f). These changes demonstrated that EUGR rats had a PAH phenotype *in vivo*.

Pulmonary artery smooth muscle cells of EUGR rats exhibited elevated cell proliferation and migration ability

Since PASMC proliferation is one of the underlying mechanisms of PAH vascular remodeling, we investigated

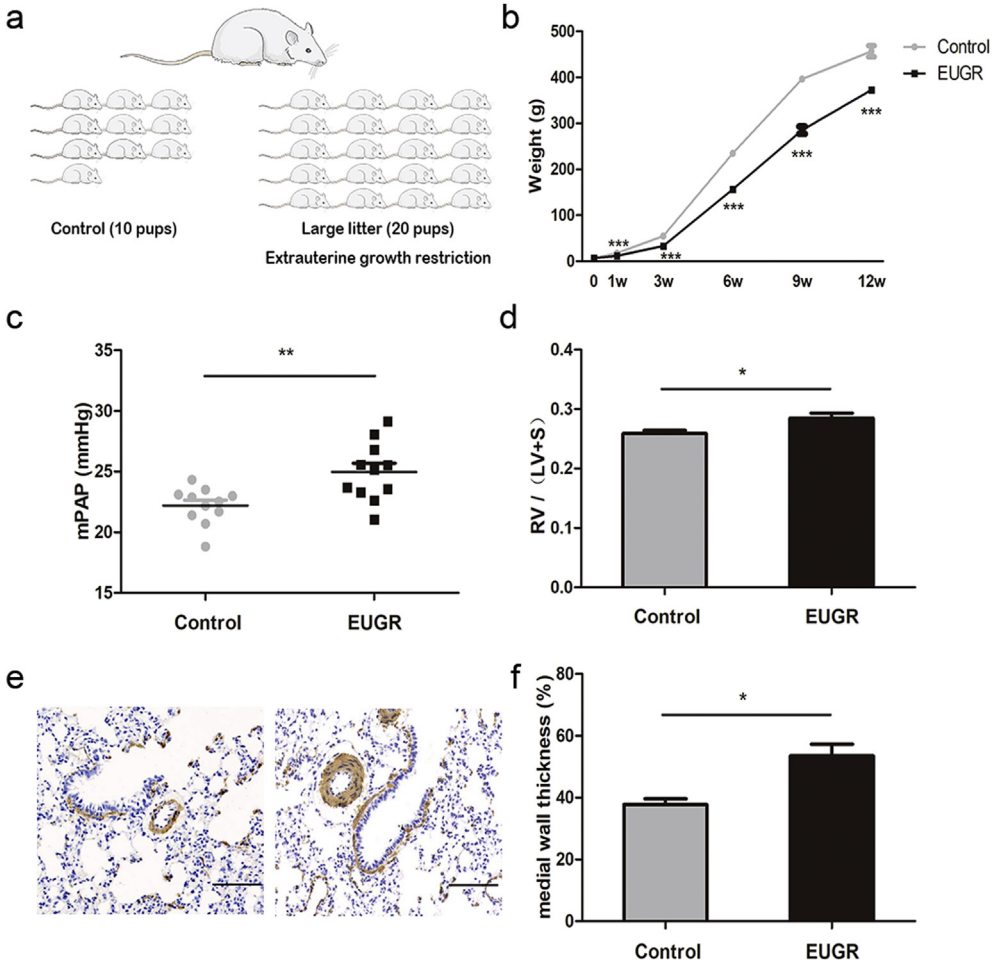

Figure 1 Extrauterine growth restriction male rats developed increased pulmonary artery pressure and pulmonary arteriolar remodeling. (a) EUGR rat model (b) Changes in body weight (g) in EUGR and control rats. $n = 25$ rats per group. $^{***}P < 0.001$ compared to control; unpaired Student's *t*-test. (c) mean Pulmonary Arterial Pressure (mPAP) (d) RV hypertrophy (RV/(LV + septum (S))) of the rats. $n = 11$ rats per group.$^{*}P < 0.05$, $^{**}P < 0.01$ compared to control; unpaired Student's *t*-test. (e) α-sma staining (representative photomicrographs are shown). Scale bars, 100 μm. (f) Medial wall thickness of pulmonary arteries in small (20–100 μm in diameter) pulmonary vessels. All data throughout the figures represent the mean ± s.e.m.

whether EUGR affected proliferation of PASMCs. The EUGR exhibited hyperproliferation (Fig. 2a) of PASMCs isolated from rats compared with control. Cell count also suggested proliferation of EUGR PASMCs (Fig. 2b). The apoptosis resistance of PASMCs was not significant (Fig. 2c and Supplementary Fig. 1a). Furthermore, we studied the migration of PASMC cells. Elevated cell migration by wound injury (Fig. 2d) and transwell assay (Fig. 2e) were found in EUGR PASMCs. These results suggested that PASMCs of EUGR had more proliferation and migration ability than those of control group, and had the characteristics of smooth muscle dysfunction in pulmonary hypertension.

Notch3 and Notch3 target genes are dysregulated in EUGR-induced PAH vessels

To study the mechanism whereby Notch signaling is activated in EUGR rat lungs, we examined the expression of Notch isoforms (encoded by Notch1, Notch2, Notch3 and Notch4) and Notch regulated genes by realtime quantitative PCR in whole lung tissues (Fig. 3a). Notably, several Notch-related ligands, receptors and target genes were dysregulated. And to determine whether the key Notch regulation occurs in the medial layer, we isolated smooth muscle cells from control and EUGR rats. Based on previous research and information, we continued to detect gene expression mainly expressed in smooth muscle. In pulmonary smooth muscle tissues, relative mRNA expression showed upregulation of Notch3 and Notch3 target gene Hey1 as compared with control (Fig. 3b). We also found elevated levels of Notch3 ICD protein and Hey1 Protein in EUGR PASMC compared to control samples (Fig. 3c and d). Immunofluorescence staining of rat lungs showed that Notch3 expression was localized in the media of pulmonary arteries. Increased Notch3 immunoreactivity was seen in EUGR compared to control (Fig. 3e). Relative mRNA expression and protein expression of Notch ligand Jag1 in smooth muscle were not significantly changed (Supplementary Fig. 1b and c). Our results indicated that Notch3 and its target gene Hey1 were upregulated and were sensitive markers in EUGR-induced PAH rat model.

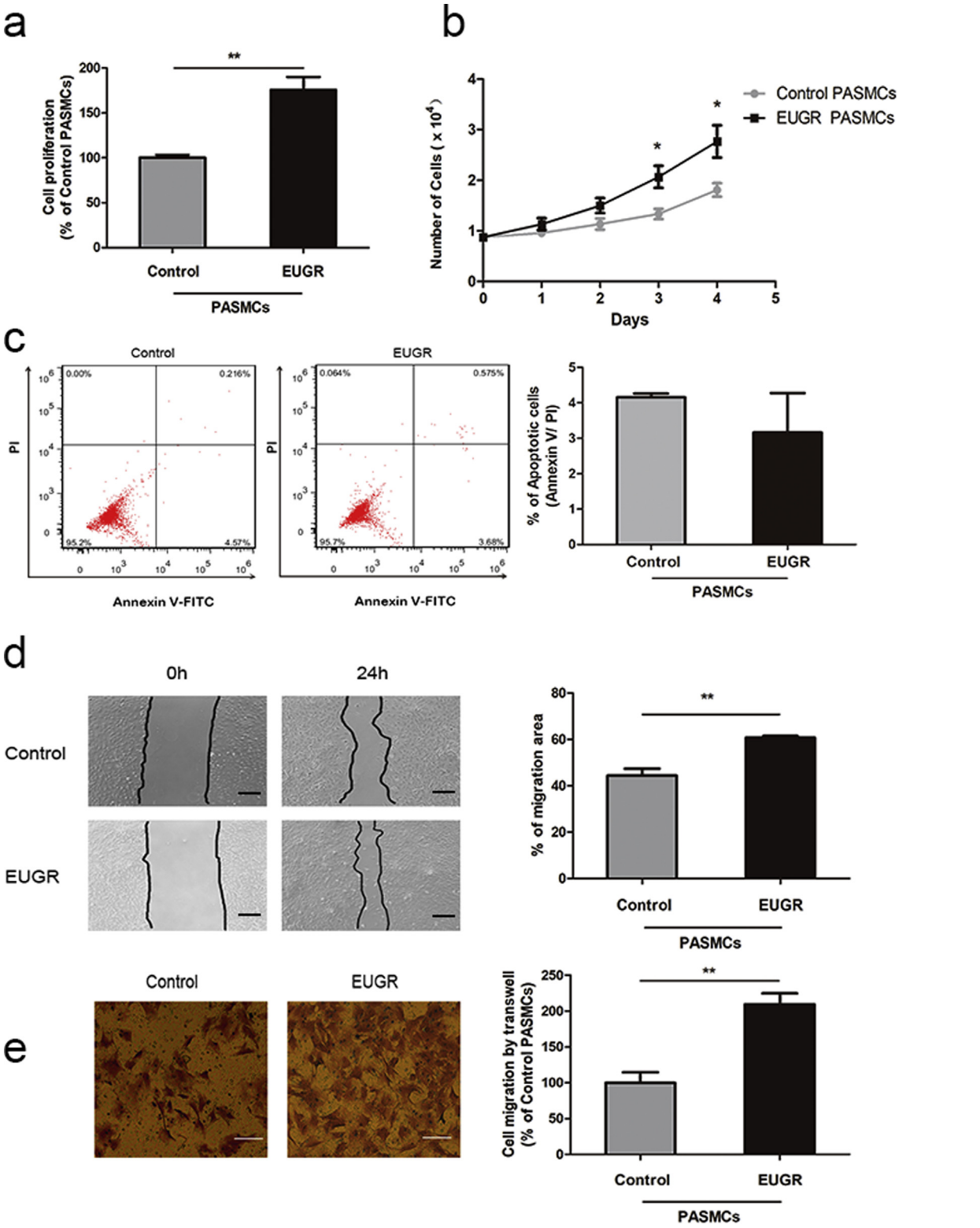

Figure 2 Pulmonary artery smooth muscle cells in EUGR rats exhibited elevated cell proliferation and migration. (a) Cell proliferation (BrdU colorimetric incorporation assay) of rat PASMCs. (b) Growth curve of rat PASMCs (c) Cell apoptosis (flow cytometry using the Annexin V/PI staining) (d) Cell migration by wound injury Scale bars, 200 μm. (e) Cell migration by transwell assay of PASMCs isolated from EUGR and control rats. Scale bars, 50 μm. The analyses shown in a–e were from subcultured PASMCs derived from four control and four EUGR rat lungs. Values are expressed as a percentage relative to control-PASMCs. $^{*}P < 0.05$, $^{**}P < 0.01$ compared to control PASMCs; unpaired Student's *t*-test. All data throughout the figures represent the mean ± s.e.m.

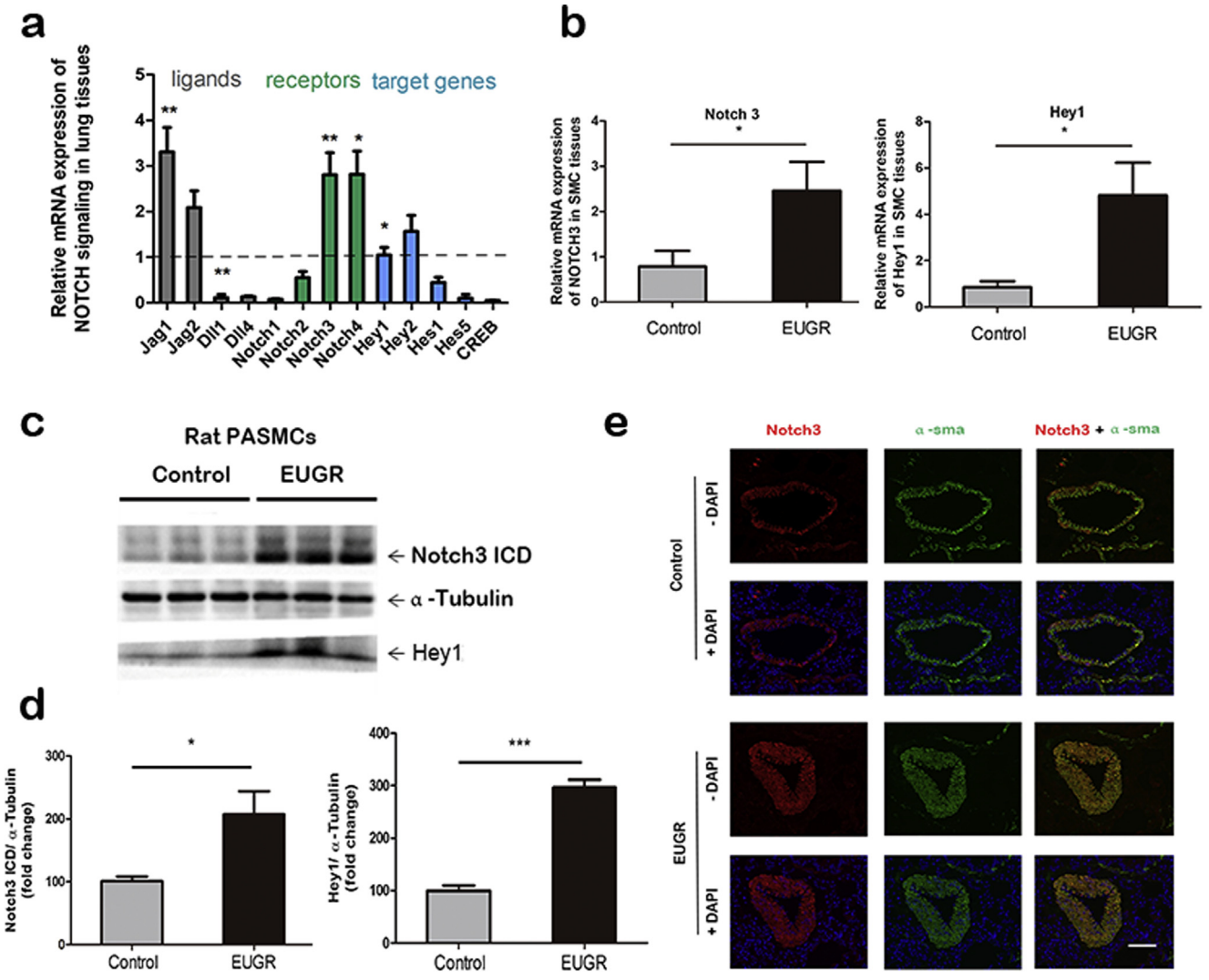

Figure 3 Notch3 upregulation in EUGR-induced PAH PASMCs. (a) Relative mRNA expression of Notch signaling ligands (DLL, JAG), Notch isoforms (Notch1−Notch4) and the indicated Notch-regulated genes from lungs of EUGR rats compared to control. Relative mRNA expression of the gene in control group was set as 1. $n = 6$ per group. $^{*}P < 0.05$, $^{**}P < 0.01$ compared to control; unpaired Student's *t*-test. (b) Relative mRNA expression of Notch3 and Hey1 in smooth muscle tissues of the lung. $n = 5$ per group in b and c. $^{*}P < 0.05$ compared to control; unpaired Student's *t*-test. (c) Western blot analysis of Notch3, Hey1 and α-Tubulin (loading control) from isolated PASMCs of three EUGR and four control per individual. The blots are representative of the three total number of runs. (d) Relative expression values obtained by densitometry of Notch3 ICD protein and Hey 1 protein normalized to α-Tubulin (loading control) ($n = 3$ per group). (e) Representative immunofluorescence photomicrographs of Notch3 (red) and α-smooth muscle actin (α-actin, a marker specific for smooth muscle cells, green) in small pulmonary arteries from rat lungs of EUGR and control. Nuclei are counterstained with DAPI (blue). Scale bars, 100 μm. The images are representative of $n = 3$ lungs per group. All data throughout the figure represent the mean ± s.e.m.

Notch signaling inhibitor DAPT treatment ameliorates EUGR PASMC proliferation

To evaluate the functional role of Notch3 in PASMCs, we treated PASMCs with the γ-secretase inhibitor DAPT (N-[N-(3,5-diflurophenacetyl)-L-alanyl]-S-phenylglycine tbutyl ester) *in vitro*, which had been shown to block the cleavage of Notch proteins to ICD peptides.

DAPT treatment of rat PASMCs led to downregulation of Notch3 and Hey1 mRNA expression (Fig. 4a and b). DAPT partially inhibited EUGR-induced increase in the protein expression of Notch3 ICD and Hey1 after DAPT treatment (Fig. 4c and d). Notably, DAPT treatment inhibited cell proliferation in a dose-dependent manner (Fig. 4e). DAPT also reduced the EUGR-induced migration of rat PASMCs (Fig. 4f). The migration index of DAPT treatment EUGR cells was decreased by 11%, 25%, 29% and 40% at 10, 25, 50, 100 μmol/L, respectively. The result of transwell assay was not significant (Fig. 4g). These results indicated that the antiproliferative effects of DAPT in PASMCs were mediated to a major extent by Notch3 reduction.

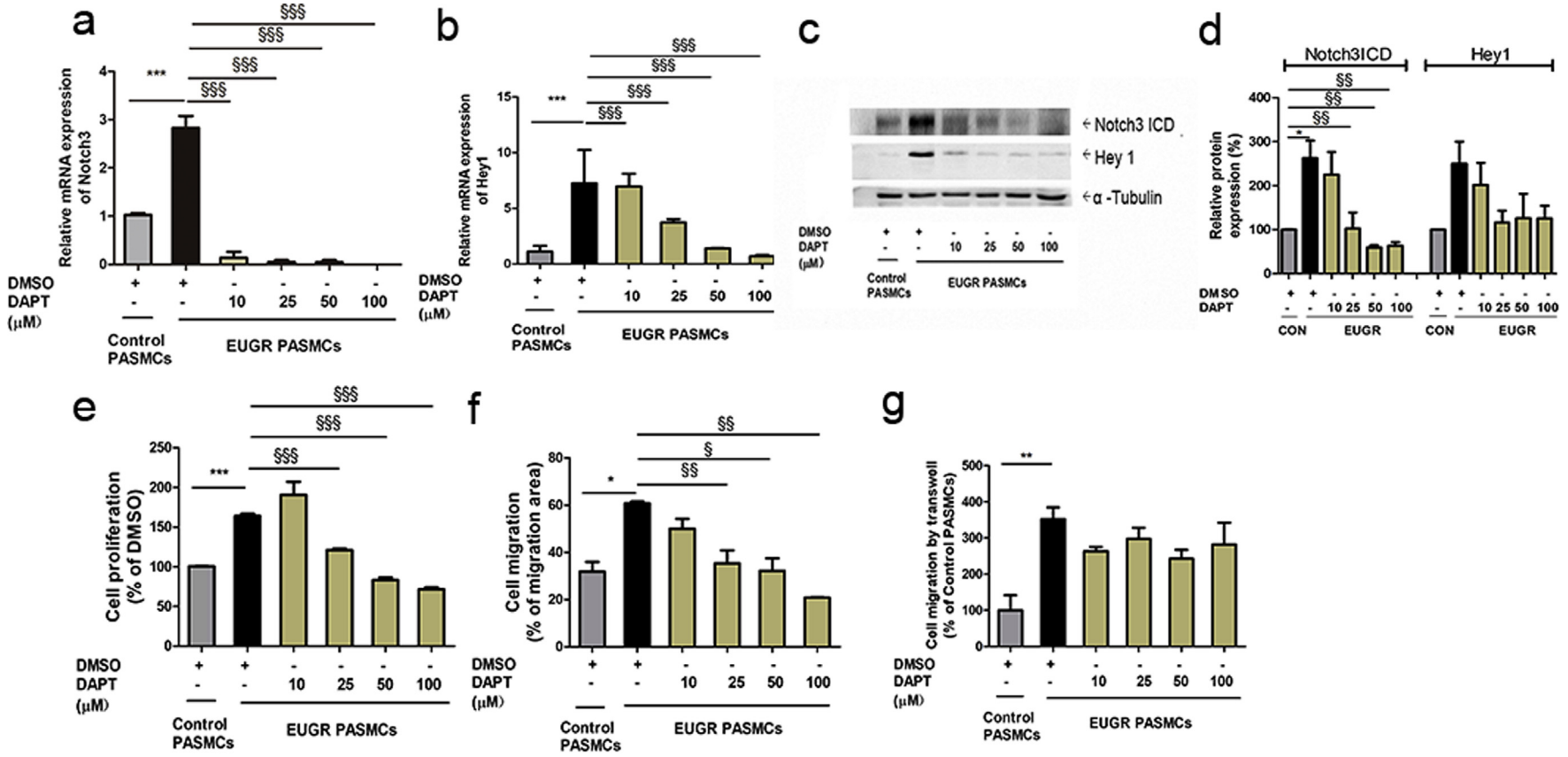

Figure 4 Notch inhibitor DAPT treatment ameliorated EUGR-induced PASMC proliferation (a, b) Relative mRNA expression of Notch3 and Hey1 after 48 h of DMSO or Notch inhibitor DAPT treatment as shown. $n = 6$ per group in A and B. $^{***}P < 0.001$ compared to control; $§§§P < 0.001$ compared to EUGR DMSO treated PASMCs; one-way analysis of variance (ANOVA) followed by Student–Newman–Keuls multiple comparison test. (c) Western blot analysis of Notch3, Hey1 and α-Tubulin (loading control) in PASMCs treated with DAPT or DMSO. The blots in c are representative of the three total number of runs. (d) Relative expression values obtained by densitometry of Notch3 ICD protein and Hey 1 protein normalized to α-Tubulin (loading control) ($n = 3$ per group). (e) Proliferation (BrdU incorporation) of PASMCs. (f) Cell migration by wound injury and (g) cell migration by transwell assay of PASMCs in the presence or absence of the Notch inhibitor DAPT or DMSO. The analyses shown in c–g were from subcultured PASMCs derived from three control and five EUGR rat lungs. Values in e and g are expressed as a percentage relative to control-PASMCs. $^{*}P < 0.05$, $^{**}P < 0.01$, $^{***}P < 0.001$ compared to control PASMCs; $§P < 0.05$, $§§P < 0.01$, $§§§P < 0.001$ compared to EUGR DMSO treated PASMCs; one-way analysis of variance (ANOVA) followed by Student–Newman–Keuls multiple comparison test. All data throughout the figure represent the mean ± s.e.m.

Knockdown of Notch3 reverses the PAH features in PASMCs

To further evaluate whether constitutive deletion of Notch3 can reverse the vascular phenotype of EUGR induced PAH, we knocked down Notch3 in rat PASMCs using lentivirus-mediated rat Notch3 shRNA transduction. Noch3 expression in PASMCs, as determined by RT-PCR, confirmed the efficacy of gene transfer (Fig. 5a). Subcultured PASMCs transducted with lentivirus-Notch3 shRNA 1# (Fig. 5b and c) and shRNA 2# (Supplement Fig. 1d and e) exhibited deletion in Notch3 ICD protein and Hey1 protein, compared with those of PASMCs transducted with scrambled shRNA. We next investigated whether knockdown of Notch3 affected the proliferation and migration of rat EUGR-PAH PASMCs. PASMCs displayed reduced proliferation after genetic ablation of Notch3 (Fig. 5d). Wound healing and transwell chamber assays revealed that migration was also less in Notch3-knockdown PASMCs than that in EUGR PASMCs transducted with scrambled shRNA (Fig. 5e and f). These results suggested that an upregulated Notch3-Hey1 signaling pathway played an important role in the proliferation and migration of PASMCs, and knockdown of Notch3 could attenuate this process.

Inhibition of Notch3 cleavage reverses PAH phenotype in vivo

To further investigate the effects of Notch3 signaling on EUGR *in vivo*, either the γ-secretase inhibitor (DAPT, 10 mg/kg/d) or dimethyl sulfoxide (DMSO) was administered to EUGR or control rats at 48 h before sacrificed at 12 weeks old. The dose was based on previous studies [15,16]. EUGR rats received this drug had significant reductions in mPAP, while EUGR rats which did not receive DAPT developed PAH with elevated mPAP (Fig. 6a). Right ventricular hypertrophy improved a part, but the statistical results were not very significant after treatment (Fig. 6b). Notably, DAPT treated rats reduced cell proliferation in PASMCs isolated from EUGR (Fig. 6c), which was consistent with the results of *in vitro* experiments. Migration of PASMCs isolated from DAPT treated EUGR rats was not significantly decreased (Fig. 6d). Although gastrointestinal and skin side effects had been reported with γ-secretase inhibitors [23,24], we observed that DAPT was well

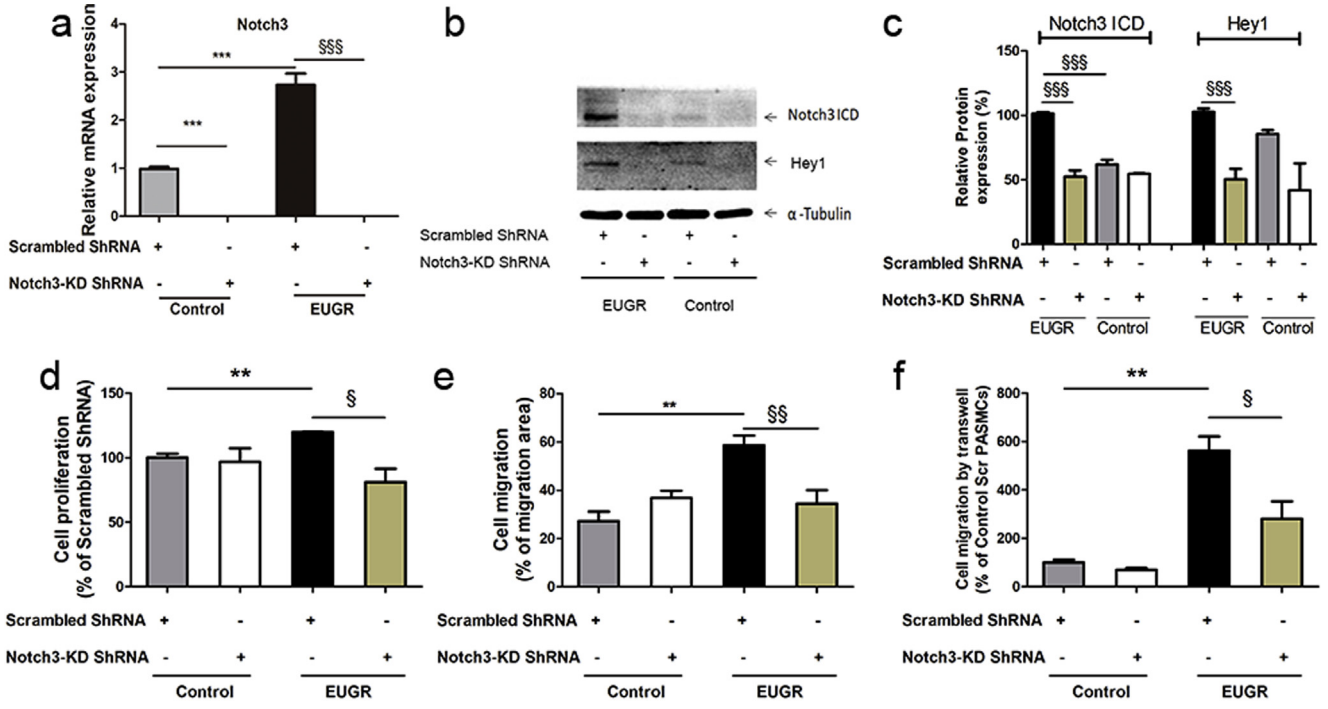

Figure 5 Targeted deletion of Notch3 in PASMCs led to reduced Notch signaling activity in PASMC cells. (a) Relative mRNA expression of Notch3 from rat PASMCs transduced with Notch3 shRNA (Notch3-KD) or scrambled shRNA (Scr) lentivirus for 48 h. $n = 6$ per group in a. $^{***}P < 0.001$ compared to Control scrambled shRNA lentivirus treated PASMCs; $§§§P < 0.001$ compared to EUGR scrambled shRNA lentivirus treated PASMCs; one-way analysis of variance (ANOVA) followed by Student–Newman–Keuls multiple comparison test. (b) Western blot analysis of Notch3, Hey1 and α-Tubulin (loading control) in PASMCs transduced with Notch3 shRNA 1# (Notch3-KD) or scrambled shRNA lentivirus. The blots in b are representative of the three total number of runs. (c) Relative expression values obtained by densitometry of Notch3 ICD protein and Hey 1 protein normalized to α-Tubulin (loading control) ($n = 3$ per group). $§§§P < 0.001$ compared to EUGR scrambled shRNA lentivirus treated PASMCs; one-way analysis of variance (ANOVA) followed by Student–Newman–Keuls multiple comparison test. (d) Proliferation (BrdU incorporation) (e) cell migration and (f) cell migration by transwell assay of PASMCs transduced with Notch3 shRNA (Notch3-KD) or scrambled shRNA (Scr) lentivirus. Values are expressed as a percentage relative to control-Scr PASMCs. The analyses shown in d–f are from subcultured PASMCs derived from three control and three EUGR rat lungs. $^{**}P < 0.01$ compared to control Scr PASMCs; $§P < 0.05$, $§§P < 0.01$ compared to EUGR scrambled shRNA lentivirus treated PASMCs; one-way analysis of variance (ANOVA) followed by Student–Newman–Keuls multiple comparison test. All data throughout the figure represent the mean ± s.e.m.

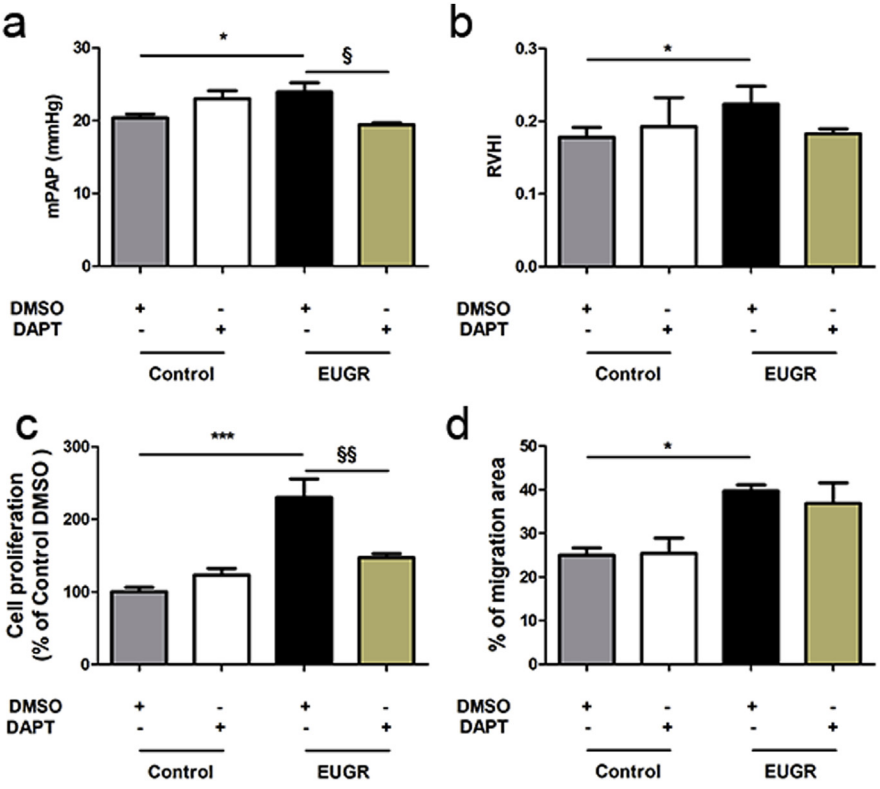

Figure 6 Inhibition of Notch3 cleavage reverses PAH phenotype *in vivo*.(a) Mean Pulmonary Arterial Pressure (mPAP) of the DAPT-treated and DMSO-treated rats. $n = 6$ rats per group.*$P < 0.05$ compared to DMSO-treated controls; §$P < 0.05$ compared to DMSO-treated EUGR; one-way analysis of variance (ANOVA) followed by Student–Newman–Keuls multiple comparison test. (b) The right ventricular hypertrophy index (RVHI) of the DAPT-treated and DMSO-treated rats. $n = 4$ per group. *$P < 0.05$ compared to DMSO-treated control rats; one-way analysis of variance (ANOVA) followed by Student–Newman–Keuls multiple comparison test. (c) Proliferation (BrdU incorporation), values are expressed as a percentage relative to DMSO-treated controls. (d) Cell migration of PASMCs isolated from rats. The analyses shown in c–d are from subcultured PASMCs derived from three control and three EUGR rat lungs. *$P < 0.05$, ***$P < 0.001$ compared to DMSO-treated controls; §§$P < 0.01$ compared to DMSO-treated EUGR; one-way analysis of variance (ANOVA) followed by Student–Newman–Keuls multiple comparison test. All data throughout the figure represent the mean ± s.e.m.

tolerated in this experiment, and no clinical symptoms of gastrointestinal tract and skin changes appeared in rats. In addition, no other clinical symptoms were observed at this dose, such as irritability, abnormal movement, and local redness and swelling. These results indicate that the therapeutic effect of DAPT on EUGR-induced PAH can improve hemodynamics and involve the anti-proliferation effect on PASMCs.

Discussion

Our goal has been to understand the molecular basis by which EUGR causes smooth muscle hyperplasia in pulmonary vasculature leading to the occluding of the distal pulmonary arterial tree and the development of PAH. The present study provides strong evidence that upregulation of Notch3 signaling in the medial layer of small pulmonary arteries is centrally involved in the adult-onset EUGR-induced PAH. This concept is based on the findings that (i) EUGR caused development of an increased mPAP in rats and enhanced PASMC proliferation and migration; (ii) Notch3 and its downstream effector, Hey1, were upregulated in EUGR rat models; (iii) pharmacological and genetic ablation of Notch3 attenuated PAH features *in vitro* and *in vivo*. Collectively, these results suggest that Notch3 signaling is required for the clinical and pathologic development of PAH. To our knowledge, these findings are the first description of PASMCs dysfunction in the EUGR-induced PAH.

Various etiologies account for PAH, including gene variants, epigenetic changes, levels of sex hormones, cardiovascular disorders, environmental and nutritional factors, and other risk factors (hypoxia, virus infection, drugs) [25–27]. During lung development, there are five stages of pulmonary maturation: embryonic (4–7 weeks); pseudoglandular (7–17 weeks); canalicular (17–26 weeks); saccular (27–36 weeks) and alveolar stages (36 weeks–2 years) [28]. Although pulmonary maturation occurs mainly during pregnancy, alveolar formation only begins around 36 weeks of gestation and lasts for up to 4 years after birth [29]. The risk factors experienced in this huge time window after birth will affect the interaction between alveolar and pulmonary vascular development. Therefore, EUGR has a certain impact on the occurrence of lung diseases.

The mechanism of EUGR-induced PAH is largely unknown. Our results suggest that EUGR is a critical factor that could induce PAH. Elevated levels of mPAP, RV

hypertrophy and vascular remodeling were demonstrated in EUGR-PAH rats (Fig. 1). As PASMC proliferation and migration were prominent features of PAH [30,31], we also demonstrated that rat PASMCs in EUGR showed an enhanced proliferation and migration features of PAH phenotype (Fig. 2).

Emerging evidence implicates Notch pathway in the pathogenesis of PAH [32–34]. In our study, Notch3 signaling was found activated in EUGR induced PAH. Notch3 was overexpressed at mRNA and protein levels (Fig. 3) in PASMCs of PAH, support a potentially role of NOTCH signaling in mediating SMC proliferation seen in this disease. The Notch3 target gene Hey1 was also significant overexpressed in PASMCs. Notch ligand Jag1 was abundantly expressed in the whole lung, but not in smooth muscle. Based on the references, we consider that Jag1 mainly plays a ligand role in endothelial cells, but not mainly in smooth muscle [35,36]. Our data provide the evidence that Notch3 regulates EUGR-PAH. Thus, Notch3 activation might provide a new therapeutic target in EUGR-PAH.

In DAPT-treated animal models and DAPT-exposed PAH PASMCs, the drug had ability to strongly reduced proliferation of PASMCs *in vitro* (Figs. 4e and 6c) and reverse the clinical features of established experimental PAH *in vivo* (Fig. 6a). We also found decreased Notch3 ICD expression and decreased downstream target gene Hey1 expression (Fig. 4a–d). Transwell chamber migration assay could indicate the ability of cells to migrate, but unlike scratch tests, it may also reflect the ability of cells invasion. So this explains that the two experimental results were not exactly the same (Fig. 4f and g). Our study offered a reversal therapy probability of DAPT that PAH could be effectively treated by blocking Notch3 signaling in this model. Future studies also need to assess the systemic side effects and efficacy of DAPT when use in childhood. In addition, further studies may consider combining DAPT with other drugs or materials to make the delivery process to the pulmonary vessels more precise.

The central role of Notch3 in the pathogenesis of PAH is further supported by *in vitro* loss-of-function studies. These data indicate that depletion of Notch3 in SMCs is sufficient to reverse the PAH phenotype of hyperproliferate and migration (Fig. 5d–f). These results further confirm that Notch3 signaling pathway is involved in the pathogenesis of EUGR-PAH by affecting the proliferation and migration of smooth muscle cells. There is a discrepancy between DAPT-treatment and Notch3 shRNA knockdown on transwell cell migration assay. Results of transwell are affected in the shRNA experiment, while they are not statistically significant in the DAPT-treatment. This may be due to the mechanism of DAPT. DAPT is a γ-secretase inhibitor, which inhibits Notch signaling by preventing intracellular cleavage of Notch receptor. It is noteworthy that DAPT inhibits Notch signaling in an indirect manner. Thus, the effect of DAPT may come from the combined inhibition of multiple substrates of γ-secretase (such as EphA4) [37–39]. In addition, DAPT is non-specific for Notch3. The smooth muscle not only expresses Notch3, but also Notch 2 [40]. Specific knockdown of Notch3 may be more accurate than DAPT for Notch3 inhibition, so we then knockdown Notch3 with lentiviral shRNA to detect its effect on cell migration.

The Notch pathway is an evolutionarily conserved signaling mechanism and plays a role in the organ development of most vertebrates [20,40] The Notch signaling pathway consists of an extensive family of complex proteins. The receptors and ligands in the family are important for the regulation of growth, apoptosis, migration, cell fate determination, and are key mediators of vascular morphogenesis [41,42]. In vascular smooth muscle cells, Notch2 and Notch3 predominate [40], while Notch1 and Notch4 are primarily present in endothelial cells [20,43]. The molecular machinery of Notch in SMC varies with different tissues or diseases, and yet incompletely understood. Recent *in vitro* studies suggest that Notch crosstalks with other pathways, such as the TGF-β signaling pathway [44–47] or the PDGF signaling pathway [48] to modulate SMC migration. Much more, however, remains to be explored within this area.

In summary, we find that high expression levels of Notch3 are associated with the development of EUGR-induced PAH. Our work demonstrates that Notch3 signaling promotes pulmonary smooth muscle cells into a proliferative phenotype. Molecular targeting of the Notch3-Hey1 axis in pulmonary vascular smooth muscle may be a useful strategy for treatment of PAH.

Author contributions

Y.W., S.X.D, L.L.Y, J.H., Q.H., X.Y.C. and Y.L. acquired the data. Y.W., S.X.D, J.H., Y.L. and L.Z.D. analyzed and interpreted the data. Y.W., S.X.D and L.Z.D. conceived and designed research. Y.W., E.P. and L.Z.D. drafted and revised the manuscript.

Conflicts of interest

The authors declare no competing interests.

Acknowledgments

This work was supported by Zhejiang Key Laboratory for Diagnosis and Therapy of Neonatal Diseases, Key Laboratory of Reproductive Genetics (Zhejiang University), Ministry of Education, and by grants from the National Natural Science Foundation of China (No. 81471480, 81630037 and 81501293).

Appendix A. Supplementary data

Supplementary data related to this article can be found at https://doi.org/10.1016/j.numecd.2019.03.004.

References

[1] Barker DJ, Osmond C. Infant mortality, childhood nutrition, and ischaemic heart disease in England and Wales. Lancet 1986; 1(8489):1077–81.

[2] Pampanini V, Boiani A, De Marchis C, Giacomozzi C, Navas R, Agostino R, et al. Preterm infants with severe extrauterine growth retardation (EUGR) are at high risk of growth impairment during childhood. Eur J Pediatr 2015;174(1):33–41. https://doi.org/10.1007/s00431-014-2361-z.
[3] Tare M, Parkington HC, Bubb KJ, Wlodek ME. Uteroplacental insufficiency and lactational environment separately influence arterial stiffness and vascular function in adult male rats. Hypertension 2012;60(2):378–86. https://doi.org/10.1161/HYPERTENSIONAHA.112.190876.
[4] Berenz A, Vergales JE, Swanson JR, Sinkin RA. Evidence of early pulmonary hypertension is associated with increased mortality in very low birth weight infants. Am J Perinatol 2017;34(8):801–7. https://doi.org/10.1055/s-0037-1598246.
[5] Marques PC, Rocha G, Flor-De-Lima F, Guimaraes H. Extrauterine growth restriction at discharge in very low birth weight infants: a retrospective study in a level III neonatal intensive care unit. Minerva Pediatr 2018. https://doi.org/10.23736/S0026-4946.18.05253-2.
[6] Nuyt AM. Mechanisms underlying developmental programming of elevated blood pressure and vascular dysfunction: evidence from human studies and experimental animal models. Clin Sci 2008;114(1):1–17. https://doi.org/10.1042/CS20070113.
[7] Wedgwood S, Warford C, Agvateesiri SC, Thai P, Berkelhamer SK, Perez M, et al. Postnatal growth restriction augments oxygen-induced pulmonary hypertension in a neonatal rat model of bronchopulmonary dysplasia. Pediatr Res 2016;80(6):894–902. https://doi.org/10.1038/pr.2016.164.
[8] Zhang L, Tang L, Wei J, Lao L, Gu W, Hu Q, et al. Extrauterine growth restriction on pulmonary vascular endothelial dysfunction in adult male rats: the role of epigenetic mechanisms. J Hypertens 2014;32(11):2188–98. https://doi.org/10.1097/HJH.0000000000000309 [discussion 98].
[9] Tang LL, Zhang LY, Lao LJ, Hu QY, Gu WZ, Fu LC, et al. Epigenetics of Notch1 regulation in pulmonary microvascular rarefaction following extrauterine growth restriction. Respir Res 2015;16:66. https://doi.org/10.1186/s12931-015-0226-2.
[10] D'Alonzo GE, Barst RJ, Ayres SM, Bergofsky EH, Brundage BH, Detre KM, et al. Survival in patients with primary pulmonary hypertension. Results from a national prospective registry. Ann Intern Med 1991;115(5):343–9.
[11] Schermuly RT, Ghofrani HA, Wilkins MR, Grimminger F. Mechanisms of disease: pulmonary arterial hypertension. Nat Rev Cardiol 2011;8(8):443–55. https://doi.org/10.1038/nrcardio.2011.87.
[12] Savai R, Al-Tamari HM, Sedding D, Kojonazarov B, Muecke C, Teske R, et al. Pro-proliferative and inflammatory signaling converge on FoxO1 transcription factor in pulmonary hypertension. Nat Med 2014;20(11):1289–300. https://doi.org/10.1038/nm.3695.
[13] He Q, Liu X, Zhong Y, Xu SS, Zhang ZM, Tang LL, et al. Arginine bioavailability and endothelin-1 system in the regulation of vascular function of umbilical vein endothelial cells from intrauterine growth restricted newborns. Nutr Metabol Cardiovasc Dis: NMCD 2018;28(12):1285–95. https://doi.org/10.1016/j.numecd.2018.09.002.
[14] Seeger W, Pullamsetti SS. Mechanics and mechanisms of pulmonary hypertension-conference summary and translational perspectives. Pulm Circ 2013;3(1):128–36.
[15] Li X, Zhang X, Leathers R, Makino A, Huang C, Parsa P, et al. Notch3 signaling promotes the development of pulmonary arterial hypertension. Nat Med 2009;15(11):1289–97. https://doi.org/10.1038/nm.2021.
[16] Wang W, Liu J, Ma A, Miao R, Jin Y, Zhang H, et al. mTORC1 is involved in hypoxia-induced pulmonary hypertension through the activation of Notch3. J Cell Physiol 2014;229(12):2117–25. https://doi.org/10.1002/jcp.24670.
[17] Roca C, Adams RH. Regulation of vascular morphogenesis by Notch signaling. Genes Dev 2007;21(20):2511–24. https://doi.org/10.1101/gad.1589207.
[18] Alva JA, Iruela-Arispe ML. Notch signaling in vascular morphogenesis. Curr Opin Hematol 2004;11(4):278–83. https://doi.org/10.1097/01.moh.0000130309.44976.ad.
[19] Collesi C, Felician G, Secco I, Gutierrez MI, Martelletti E, Ali H, et al. Reversible Notch1 acetylation tunes proliferative signalling in cardiomyocytes. Cardiovasc Res 2018;114(1):103–22. https://doi.org/10.1093/cvr/cvx228.
[20] Fouillade C, Monet-Lepretre M, Baron-Menguy C, Joutel A. Notch signalling in smooth muscle cells during development and disease. Cardiovasc Res 2012;95(2):138–46. https://doi.org/10.1093/cvr/cvs019.
[21] des Robert C, Li N, Caicedo R, Frost S, Lane R, Hauser N, et al. Metabolic effects of different protein intakes after short term undernutrition in artificially reared infant rats. Early Hum Dev 2009;85(1):41–9. https://doi.org/10.1016/j.earlhumdev.2008.06.009.
[22] Clark RH, Thomas P, Peabody J. Extrauterine growth restriction remains a serious problem in prematurely born neonates. Pediatrics 2003;111(5 Pt 1):986–90.
[23] Stanger BZ, Datar R, Murtaugh LC, Melton DA. Direct regulation of intestinal fate by Notch. Proc Natl Acad Sci U S A 2005;102(35):12443–8. https://doi.org/10.1073/pnas.0505690102.
[24] Imbimbo BP, Giardina GA. gamma-secretase inhibitors and modulators for the treatment of Alzheimer's disease: disappointments and hopes. Curr Top Med Chem 2011;11(12):1555–70.
[25] Wang Y, Yan L, Zhang Z, Prado E, Fu L, Xu X, et al. Epigenetic regulation and its therapeutic potential in pulmonary hypertension. Front Pharmacol 2018;9:241. https://doi.org/10.3389/fphar.2018.00241.
[26] Gamen E, Seeger W, Pullamsetti SS. The emerging role of epigenetics in pulmonary hypertension. Eur Respir J 2016;48(3):903–17. https://doi.org/10.1183/13993003.01714-2015.
[27] Xu XF, Ma XL, Shen Z, Wu XL, Cheng F, Du LZ. Epigenetic regulation of the endothelial nitric oxide synthase gene in persistent pulmonary hypertension of the newborn rat. J Hypertens 2010;28(11):2227–35. https://doi.org/10.1097/HJH.0b013e32833e08f1.
[28] Kumar VHS. Diagnostic approach to pulmonary hypertension in premature neonates. Children 2017;4(9). https://doi.org/10.3390/children4090075.
[29] Kumar VH, Lakshminrusimha S, El Abiad MT, Chess PR, Ryan RM. Growth factors in lung development. Adv Clin Chem 2005;40:261–316.
[30] Nakanishi N, Ogata T, Naito D, Miyagawa K, Taniguchi T, Hamaoka T, et al. MURC deficiency in smooth muscle attenuates pulmonary hypertension. Nat Commun 2016;7:12417. https://doi.org/10.1038/ncomms12417.
[31] Lv Y, Tang LL, Wei JK, Xu XF, Gu W, Fu LC, et al. Decreased Kv1.5 expression in intrauterine growth retardation rats with exaggerated pulmonary hypertension. Am J Physiol Lung Cell Mol Physiol 2013;305(11):L856–65. https://doi.org/10.1152/ajplung.00179.2013.
[32] Hurst LA, Dunmore BJ, Long L, Crosby A, Al-Lamki R, Deighton J, et al. TNFalpha drives pulmonary arterial hypertension by suppressing the BMP type-II receptor and altering NOTCH signalling. Nat Commun 2017;8:14079. https://doi.org/10.1038/ncomms14079.
[33] Liu H, Zhang W, Kennard S, Caldwell RB, Lilly B. Notch3 is critical for proper angiogenesis and mural cell investment. Circ Res 2010;107(7):860–70. https://doi.org/10.1161/CIRCRESAHA.110.218271.
[34] Smith KA, Voiriot G, Tang H, Fraidenburg DR, Song S, Yamamura H, et al. Notch activation of Ca(2+) signaling in the development of hypoxic pulmonary vasoconstriction and pulmonary hypertension. Am J Respir Cell Mol Biol 2015;53(3):355–67. https://doi.org/10.1165/rcmb.2014-0235OC.
[35] Liu H, Kennard S, Lilly B. NOTCH3 expression is induced in mural cells through an autoregulatory loop that requires endothelial-expressed JAGGED1. Circ Res 2009;104(4):466–75. https://doi.org/10.1161/CIRCRESAHA.108.184846.
[36] Cao Z, Lis R, Ginsberg M, Chavez D, Shido K, Rabbany SY, et al. Targeting of the pulmonary capillary vascular niche promotes lung alveolar repair and ameliorates fibrosis. Nat Med 2016;22(2):154–62. https://doi.org/10.1038/nm.4035.
[37] Sha L, Wu X, Yao Y, Wen B, Feng J, Sha Z, et al. Notch signaling activation promotes seizure activity in temporal lobe epilepsy. Mol Neurobiol 2014;49(2):633–44. https://doi.org/10.1007/s12035-013-8545-0.
[38] Xu B, Li S, Brown A, Gerlai R, Fahnestock M, Racine RJ. EphA/ephrin-A interactions regulate epileptogenesis and activity-

dependent axonal sprouting in adult rats. Mol Cell Neurosci 2003; 24(4):984–99.
[39] Matsui C, Inoue E, Kakita A, Arita K, Deguchi-Tawarada M, Togawa A, et al. Involvement of the gamma-secretase-mediated EphA4 signaling pathway in synaptic pathogenesis of Alzheimer's disease. Brain Pathol 2012;22(6):776–87. https://doi.org/10.1111/j.1750-3639.2012.00587.x.
[40] Baeten JT, Lilly B. Notch signaling in vascular smooth muscle cells. Adv Pharmacol 2017;78:351–82. https://doi.org/10.1016/bs.apha.2016.07.002.
[41] Morrow D, Sweeney C, Birney YA, Cummins PM, Walls D, Redmond EM, et al. Cyclic strain inhibits Notch receptor signaling in vascular smooth muscle cells in vitro. Circ Res 2005;96(5):567–75. https://doi.org/10.1161/01.RES.0000159182.98874.43.
[42] Sakata Y, Xiang F, Chen Z, Kiriyama Y, Kamei CN, Simon DI, et al. Transcription factor CHF1/Hey2 regulates neointimal formation in vivo and vascular smooth muscle proliferation and migration in vitro. Arterioscler Thromb Vasc Biol 2004;24(11):2069–74. https://doi.org/10.1161/01.ATV.0000143936.77094.a4.
[43] Varadkar P, Kraman M, Despres D, Ma G, Lozier J, McCright B. Notch2 is required for the proliferation of cardiac neural crest-derived smooth muscle cells. Dev Dynam 2008;237(4):1144–52. https://doi.org/10.1002/dvdy.21502.
[44] Kurpinski K, Lam H, Chu J, Wang A, Kim A, Tsay E, et al. Transforming growth factor-beta and notch signaling mediate stem cell differentiation into smooth muscle cells. Stem Cells 2010;28(4):734–42. https://doi.org/10.1002/stem.319.
[45] Blokzijl A, Dahlqvist C, Reissmann E, Falk A, Moliner A, Lendahl U, et al. Cross-talk between the Notch and TGF-beta signaling pathways mediated by interaction of the Notch intracellular domain with Smad3. J Cell Biol 2003;163(4):723–8. https://doi.org/10.1083/jcb.200305112.
[46] Bai G, Sheng N, Xie Z, Bian W, Yokota Y, Benezra R, et al. Id sustains Hes1 expression to inhibit precocious neurogenesis by releasing negative autoregulation of Hes1. Dev Cell 2007;13(2):283–97. https://doi.org/10.1016/j.devcel.2007.05.014.
[47] Kluppel M, Wrana JL. Turning it up a Notch: cross-talk between TGF beta and Notch signaling. Bioessays 2005;27(2):115–8. https://doi.org/10.1002/bies.20187.
[48] Jin S, Hansson EM, Tikka S, Lanner F, Sahlgren C, Farnebo F, et al. Notch signaling regulates platelet-derived growth factor receptor-beta expression in vascular smooth muscle cells. Circ Res 2008; 102(12):1483–91. https://doi.org/10.1161/CIRCRESAHA.107.167965.